Hindawi
Advances in Polymer Technology
Volume 2019, Article ID 7632873, 12 pages
https://doi.org/10.1155/2019/7632873

Research Article

One-Step Formation of Chondrocytes through Direct Reprogramming via Polysaccharide-Based Gene Delivery

Qingtong Yu, Yan Wang, Xia Cao, Wenwen Deng, Michael Adu Frimpong, Jiangnan Yu, and Ximing Xu

Department of Pharmaceutics, School of Pharmacy and Center for Drug/Gene Delivery and Tissue Engineering, Jiangsu University, China

Correspondence should be addressed to Jiangnan Yu; yjn@ujs.edu.cn and Ximing Xu; xmxu@ujs.edu.cn

Received 2 January 2019; Revised 17 March 2019; Accepted 8 April 2019; Published 29 May 2019

Academic Editor: Lucia Baldino

An innovative strategy for the generation of chondrocytes was thoroughly studied in this paper. Polyetherimide-modified polysaccharides of *Porphyra yezoensis* (pmPPY) served as a nonviral gene vector and delivered Sox9 plasmid to directly reprogram mouse embryonic fibroblasts into chondrocytes. The gene transfer efficiency was evaluated through ELISA, RT-PCR, and Western blot. The induced chondrocytes were identified through toluidine blue, Safranin O, and the immunostaining. The expression level of collagen II was finally evaluated through western blot. The pSox9/pmPPY nanoparticles (1:50) showed lower cytotoxicity as well as greater gene transfection efficiency than Lipofectamine 2000 and polyetherimide (PEI) ($p<0.05$). The results of toluidine blue, Safranin O, and the immunostaining of collagen II further showed that the normal MEFs were successfully reprogrammed into chondrocytes. These findings indicate that pmPPY could be a promising gene vector for the generation of chondrocytes via single-gene delivery strategy, which might provide abundant chondrocytes for cartilage repair.

1. Introduction

With the development of regenerative medicine and cell therapy, tissue repair and regeneration have made great progresses during the past decades. Embryonic stem cells (ESCs) were once extensively used in the generation of some somatic cells for their incomparable ability of three germ layers' differentiation. However, the inevitable ethical considerations should be taken into account before clinical application. In 2006, a milestone work completed by Yamanaka and collaborators changed this situation [1]. Induced pluripotent stem cells (iPSCs), which possess admirable totipotentiality in vitro, are expected to be new seed cells for tissue engineering and cell therapy. Later, some human somatic cells like chondrocytes [2], hepatocytes [3], nephrocytes [4], islet cells [5], neural cells [6], and cardiac cells [7] were successfully generated from human iPSCs. Nevertheless, the conversion of original somatic cells to various target cell lines through iPSCs is time-consuming. Therefore, direct reprogramming became a candidate strategy, which is timesaving and convenient in cell therapy applications. The employment of several gene cocktails, such as Gata4, Mef2c, Tbx5 [8] and Oct4, Sox2, Klf4, and c-Myc [9], gave rise to the generation of cardiomyocytes. A similar progress has also been made in neuroscience [10]. However, little progress has been achieved in the generation of chondrocytes through direct reprogramming. Therefore, a simple, safe and efficient way of direct reprogramming is still needed for the generation of chondrocytes.

Efficient gene delivery system is vital for direct reprogramming [11]. To this end, the cationic polysaccharides are considered to be the most attractive candidates among other gene carriers applied in gene transfection. Compared to viral vectors, these materials are natural, nontoxic, biocompatible, and biodegradable, and they can be modified easily to obtain improved physicochemical properties [12]. Particularly, some polysaccharides extracted from homologous plant food medicine were taken into consideration for the low cytotoxicity and multiple biological activities [13–15].

The objective of this study was to directly reprogram mouse embryonic fibroblasts (MEFs) into chondrocytes through cationic polysaccharide-gene nanoparticles

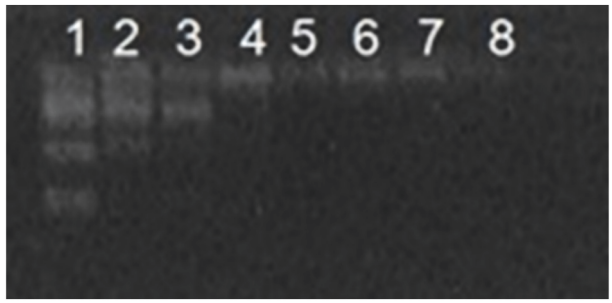

Figure 1: Electrophoretic mobility of *pmPPY-pSox9 nanoparticles* at various ratios: Lane1: Free plasmid Sox9; Lane (2-8): pmPPY/pSox9 nanoparticles in ratios of 3:1, 9:1, 15:1, 50:1, 100:1, 150:1, and 200:1.

transfection. MEFs have been extensively used in cell lines differentiation in tissue engineering as seed cells [16]. Increasing evidence indicates that the transcription factor Sox9 (a member of the Sox (Sry-type HMGbox) proteins family) plays an essential role in chondrogenesis [17, 18]. The Sox9 intriguingly regulates the formation of many types of cells, tissues, and organs like hair follicles, chondrocytes, testis, heart, lung, and central nervous system [19]. It has also been mechanistically proven to prevent chondrocytes hypertrophy with a redifferentiation effect on osteoarthritic chondrocytes which have been dedifferentiated [20, 21]. Recent reports have shown that Sox9 gene transfer could promote chondrogenesis repair *in vivo*; however, its major vehicular agent is adenoviruses which could potentiate the carrying of exogenous gene [22]. Therefore, it has become very prudent to develop safer and more effective vehicle for transferring Sox9. The novelty of this study is that, for the first time, we established a single-gene, nonviral gene delivery system for the generation of chondrocytes through the direct reprogramming strategy, which might provide a new source of chondrocytes and then facilitate the effective utilizations of *Porphyra yezoensis* polysaccharide in tissue engineering and regenerative medicine.

2. Materials and Methods

2.1. Materials. Chemical reagents were purchased from Sinopharm Chemical Reagent Co. Ltd. (Shanghai, China) while plasmid Sox9 was obtained from Public Protein/Plasmid Library (details were provided in supplementary Figure 1). Mouse embryo fibroblast (MEF), specifically 3T6 cell line, was purchased from Cell Biology (Shanghai, China). DMEM/HIGH GLUCOSE medium was procured from HyClone (Cat no. SH30243.01), China, while Gibco, USA, provided the fetal bovine serum (FBS) and penicillin/streptomycin (P/S). Agarose was obtained from Bio-WEST, Spain. Ethidium bromide was bought from Beyotime, China. The loading buffer was obtained from Takara, Japan. Moreover, DMSO was bought from MP Biomedicals (LLC, USA) while PEI was obtained from Sigma, USA. The plasmid Sox9 was purchased from Biogot Technology, Co., Ltd. (Nanjing, China). Lipofectamine 2000 was acquired from Invitrogen (Carlsbad, CA, USA) with TRIzon reagent being bought from CWBIO, China. Lastly, Dexamethasone was obtained from J&K, Beijing, China, while Safranin O and methylene blue staining were obtained from Beyotime, China.

2.2. Cell Lines. The cells were cultured in 100 mm dish of DMEM/HIGH GLUCOSE medium supplemented with 1% penicillin/streptomycin (p/s) and 10% heat-inactivated fetal bovine serum (FBS) at 37°C in a humidified atmosphere with 5% CO_2 (Thermo, USA).

2.3. Preparation of pm-PPY. In this study, pmPPY was prepared in our laboratory as described in our previous studies [23, 24]. Details can be found in supplementary information.

2.4. Preparation of pmPPY-pSox9 Nanoparticles. Briefly, 4mg pmPPY was dissolved in 2ml double distilled water (DDW) to obtain a working solution (2mg/ml). The solution was sterilized by heating at 80°C for 4h. The working solutions containing different amount of pmPPY were prepared by DMEM/high glucose medium. Subsequently, the working plasmid Sox9 solution (20μg/ml) was also prepared with 10 mM PBS (pH 7.4). However, aliquots (100μl) of both pmPPY and pSox9 working stocks were heated, respectively, at 55°C for 0.5h. Equal volumes of these two solutions were immediately mixed together and vortexed for 30s followed by incubation at room temperature for 30 min to obtain pmPPY-pSox9 nanoparticles with different pmPPY/pSox9 weight ratios.

2.5. Electrophoresis of pmPPY-pSox9 Nanoparticles. The electrophoresis was used to investigate the combination of pmPPY and plasmid DNA. For each sample, 15μl was added to 3μl of loading buffer (0.1% sodium dodecyl sulfate, 5% glycerol, and 0.005% bromophenol) and applied to a 1% agarose gel in a tris/borate/EDTA buffer solution (TBE, pH 8.0) containing 0.1mg/mL ethidium bromide. The naked plasmid Sox9 (200ng per well) was combined with pmPPY in different weight ratios (1:3, 1:9, 1:15, 1:50, 1:100, 1:150, 1:200). The free plasmid DNA served as negative control while the gel was observed under an UV transilluminator (Gel Doc 2000, Bio-rad laboratories, Hercules, CA).

2.6. Cytotoxicity Assay. The cytotoxicity of pmPPY-pSox9 nanoparticles with different weight ratios was evaluated through MTT test. Briefly, the MEFs (20,000 cells/well) were seeded in 96-well plates and incubated at 37°C (5% CO_2). The culture medium was subsequently replaced with serum-free medium for serum starvation after cell adherence to obtain a better gene transfer efficiency [25]. After 12h of serum-free incubation, pmPPY-pSox9 nanoparticles (9:1, 15:1, 30:1, 50:1, 100:1, 150:1, 200:1, and 300:1) were transferred, and the Lipofectamine 2000-Sox9 and PEI-Sox9 groups (multiple dilutions of PEI with PBS: 100-fold, 200-fold, 250-fold, 350-fold, 500-fold, 1000-fold, and 2000-fold) were used as positive controls according to the manufacturer's protocol under the same conditions. After 72 h of incubation, the supernatant in each well was replaced by 20 μl of MTT solution prepared

with PBS (5 mg/ml) followed by 4 h incubation at 37°C. Finally, 150 μl of dimethyl sulfoxide (DMSO) was added in each well to terminate the reaction. The viability percentage was relative to untreated cells. The cell viability (%) was calculated by the formula: cell viability (%) = [Abssample] / [Abscontrol] ×100. The absorption at 570nm was measured under a microplate spectrophotometer (Epoch, BioTek, USA). All the tests were carried out in triplicate.

2.7. Instrumentation and Characterization. Transmission electron microscopy (TEM) (JEM2100, JEOL, Tokyo, Japan) was used to investigate the size and shape of the nanoparticles. Briefly, 1μL of nanoparticle suspension was applied to a copper screen and air-dried. The air-dried samples were then observed directly under TEM. The surface charge and average particle size was measured using Zeta-sizer instrument (90 Plus PALS, Brookhaven, USA).

2.8. Gene Transfection Efficiency. The MEFs were seeded on 24-well plates at a density of 4×10^4 cells per well. The cells were cultured in DMEM/HIGH GLUOSE medium containing 10% FBS and incubated at 37°C (5% CO2). At about 12h after seeding, when the confluence reached 80-90%, the medium was then replaced with serum-free product for another 12h before transfection.

2.8.1. Gene Transfection. Based on electrophoresis and cytotoxicity assay, 500μl of different pmPPY-pSox9 nanoparticle suspensions (pSox9 800ng/well) prepared in 4 different pmPPY: pSox9 weight ratios (15:1, 30:1, 50:1, 100) was added into each well. The medium was replaced with fresh medium of DMEM/HIGH GLUOSE (containing 10% FBS) at 4h after transfection. In order to obtain considerable gene transfection efficiencies, the plates were incubated for 48h. For positive and negative control groups, the cells were separately treated as follows: (a) untreated; (b) pSox9 alone; (c) pSox9 plus PEI (25kDa, 2000-fold dilution); and (d) pSox9 plus Lipofectamine 2000. In addition, plasmid that encodes GFP was also transferred to MEFs under the same conditions. To investigate the level of Sox9 protein, the medium was collected 48 h after transfection and stored at -20°C for ELISA test. The extracted RNA from MEFs was also stored at -20°C for the real-time PCR experiment.

2.8.2. ELISA and RT-PCR Assay for Sox9 Expression. To investigate the transfection effect of pmPPY-pSox9 nanoparticles, the supernatant was measured according to the protocol of Human Sox9 ELISA KIT (Yantai Science and Biotechnology Co. Ltd., Yantai, China). The data were calculated based on the standard curve (y=0.0017x-0.0178, R^2=0.99936, LOD: 75pg/mL). Meanwhile, total RNA was extracted using TRIzon reagent. First-strand reverse transcription was performed using the PrimeScript™ RT Master Mix (Perfect Real Time, TakaRa, Japan). The instructions for each protocol were followed accordingly as provided by the manufacturers. The expression of SOX9 was measured using SYBR Premix Ex Taq™ (TakaRa, Japan) on a Roche lightcycler 96 Real-Time PCR System (Roche, USA). The samples were amplified under the following conditions: 94°C for 30s, followed by 40 cycles of 94°C for 5s, 58°C for 15s, and 72°C for 10s. The primer sequences (Sangon Biotech (Shanghai) Co., Ltd.) were as follows: SOX9 Forward: aggaagtcggtgaagaacgg; Sox9 Reverse: aagtcgatagggggctgtct; GAPDH Forward: agaaggctggggctcatttg; GAPDH Reverse: aggggccatccacagtcttc. All the experiments were carried out in triplicate.

2.8.3. Western Blot Test for Sox9 Expression. The treated cells in 6-well plate at a density of 2×10^5 cells/well were washed with PBS and lysed in the radioimmunoprecipitation assay (RIPA) buffer (50 Mm Tris-HCl, PH7.4, 1% Np-40, 0.25 sodium deoxycholate, 150 mM NaCl, and 1mM EDTA). The purified supernatant solution containing the proteins was obtained using centrifugation. The proteins were separated by 10% (w/v) sodium dodecyl sulfate polyacrylamide gel electrophoresis (SDS-PAGE) and transferred to poly(vinylidene fluoride) (PVDP) membranes (Millipore, USA). The resulting products were blocked with 5% nonfat milk. The membranes were incubated with mouse anti-GAPDH antibody (1:500, Sigma, USA) and rabbit anti-Sox9 antibody (1:400, Abcam, USA) separately for 2h at 37°C. After that, it was incubated with goat anti-mouse and mouse anti-rabbit HRP-conjugated secondary antibodies (1:5000, both from Santa Cruz) for 1h at 37°C, respectively. Then, the membranes were washed in Tris-Buffered Saline/Tween (TBST) and developed using Immobile Western Chemiluminescent HRP Substrate (Millipore, USA). Protein bands were visualized using a Pierce Eclipse Plus substrate (Thermo Fisher Scientific) and scanned with a ChemiScope 3200 mini (Shanghai CLinx Science Instruments Co. Ltd., Shanghai, China). ImageJ (version 4.0) was used to calculate the grey value (GV). The result was evaluated by relative expression based on the formulation: relative expression=GV_{Sox9}/GV_{GAPDH}.

2.9. Induction of Chondrocyte-Like Cells. For direct reprogramming of MEFs to chondrocytes, 1×10^4/well 3T6 cells were seeded in 6-well plates (Corning, USA) and transfected every 2 days with pmPPY-pSox9 nanoparticles. After 4 times of transfection, the cells were maintained in chondrocyte differentiation medium (CDM) (DMED/HIGH GLUCOSE, 10% FBS, 1% P/S, 1mgml^{-1} Dexamethasone (J&K, Beijing), 40 Uml^{-1} Insulin, 0.25 gml^{-1} Vitamin C, 10 ngml^{-1} basic fibroblast growth factor (bFGF) (Pepro Tech), and 10 ngml^{-1} Epidermal growth factor (EGF) (Pepro Tech)) [26–29]. The medium was changed every 3 days during the experimental period and the cell morphology was observed accordingly.

2.9.1. Staining Analysis. Safranin O and methylene blue staining were carried out to assess proteoglycans in accordance with the respective manufacturer's protocol. Type II collagen immunofluorescence was employed to detect differentiation. The cells were treated with specific cartilage medium for 14 days since the last transfection and fixed in 4% paraformaldehyde at 4°C overnight. This was immediately followed by a quick wash in PBS. After that, the product was incubated for 30 min in 5% BSA (m/v) with Triton to block unspecific

binding and to break the membrane. The primary rabbit-anti-collagen type II antibody (Abcam (ab185430), USA) was applied for 12h at 4°C. The cells were washed 3 times in PBS (5min each), followed by adding corresponding secondary antibody (sigma, USA) for 120 min at room temperature. The cells were washed twice with PBS. The MEF cells treated with pm-PPY alone were employed as negative control under the same conditions. Photomicrographs were taken with a Zeiss Axioskop 40 microscope equipped with a Zeiss AxioCam Mrc digital camera and Zeiss AxioVision software (Zeiss, Oberkochen, Germany).

2.9.2. Western Blot Analysis. The sample preparation and SDS electrophoresis protocols were the same as Section 2.8.3. The membranes were incubated with mouse anti-GAPDH antibody (1:500, Sigma, USA) and rabbit- anti-collagen type II antibody (Abcam (ab185430), USA) separately for 2h at 37°C. After that, it was incubated with goat anti-mouse and mouse anti-rabbit HRP-conjugated secondary antibodies (1:5000, both from Santa Cruz) for 1h at 37°C, respectively. Then, the membranes were washed in Tris-Buffered Saline/Tween (TBST) and developed using Immobile Western Chemiluminescent HRP Substrate (Millipore, USA). Protein bands were visualized using a Pierce Eclipse Plus substrate (Thermo Fisher Scientific) and scanned with a ChemiScope 3200 mini (Shanghai CLinx Science Instruments Co. Ltd., Shanghai, China). ImageJ (version 4.0) was used to calculate the grey value (GV). The result was evaluated by relative expression based on the formulation: relative expression=GV_{col2}/GV_{GAPDH}.

2.9.3. Glycosaminoglycan (GAG) Production Assay. Samples at each time point were harvested separately and digested using a proteinase K solution for 16 h at 60°C. With Hoechst 33258 dye staining, the DNA production was measured through a spectrofluorometer at 460 nm to determine the absorbance value. Meanwhile, the GAG production was measured using a 1,9-dimethylmethylene blue (DMMB) (Sigma, USA) assay at 525 nm. GAG production was normalized to the DNA content.

2.9.4. Reprogramming Efficiency Assay. In this study, flow cytometry was carried out to evaluate chondrocytes conversion efficiency. Collagen II (Abcam 185430, USA) was also selected as a marker to evaluate the reprogramming efficiency.

2.10. Statistical Analysis. All values were presented as mean ± SD for three measurements with statistical significance evaluated via one-way ANOVA using Graphpad Prism (Version 6.0). Differences were considered to be statistically significant when $P < 0.05$.

3. Results

3.1. Elemental Analysis and 1H-NMR Assay. Beside the characterization of pmPPY in our previous paper, elemental analysis and 1H-NMR were also carried out to determine the modification of PPY. The result of elemental analysis (USA, Perkin Elmer PE 2400 Series II) showed that the content of nitrogen in the Ed-PYP was 3.77% compared to 1.79% in PPY. The 1H-NMR spectrum for the pmPPY showed that the singlet peak at 5.1ppm was linked to the proton in the functional group –HN-CO of the pmPPY (Supplementary Figure 2).

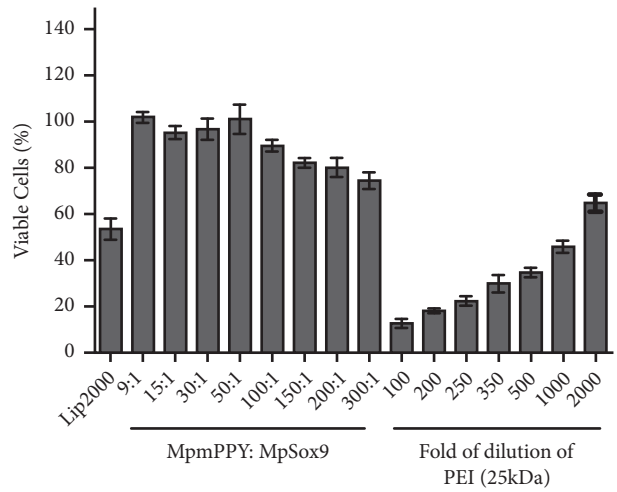

Figure 2: Cytotoxicity assay. *Notes.* Bar1, Lipofectamine 2000-(Lip2000-) plasmid Sox9 (pSox9); bar 2-9, pmPPY/pSox9 nanoparticles at various weight ratio of 9:1, 15:1, 30:1, 50:1, 100:1, 150:1, 200:1, and 300:1; bar 10-16, different folds of dilution of PEI plus pSox9, 100-, 200-, 250-, 350-, 500-, 1000-, 2000-folds from left to right.

3.2. Atomic Force Microscope (AFM) Assay. AFM assay was carried out to identify the morphology of pmPPY. Generally, the diameter of polysaccharide molecular chain is between 0.1 nm and 1 nm. In supplementary Figure 3, many spherical and lumps are evenly distributed in the images of pmPPY. The height of branched chains of pmPPY ranged from 0.2 nm to 1.0 nm. This result indicated that the construction of carbohydrate chains of pmPPY is not complicated. This property might contribute to gene release from pmPPY-based nanoparticles after cellular uptake [30]. In addition, long carbohydrate chains might cause strong immune response when they adhere to cellular membrane [31]. So the length or the complexity of polysaccharide chains should be taken into consideration during the preparation of polysaccharide-based gene vectors.

3.3. Electrophoresis. In the electrophoresis analysis, the amount of plasmid used was constant (200 ng per well) for all the lanes. As shown in Figure 1, Lanes 2–8 revealed the migration of pmPPY/pSox9 nanoparticles in different ratios of 1:3, 1:9, 1:15, 1:50, 1:100, 1:150, and 1:200, respectively. With progressive increase in pmPPY, the migration ability of DNA was significantly retarded as compared to the free plasmid Sox9 (Lane 1). The complete inhibition of plasmid migration also started from Lane 4 (1:15 ratio of pSox9/pmPPY).

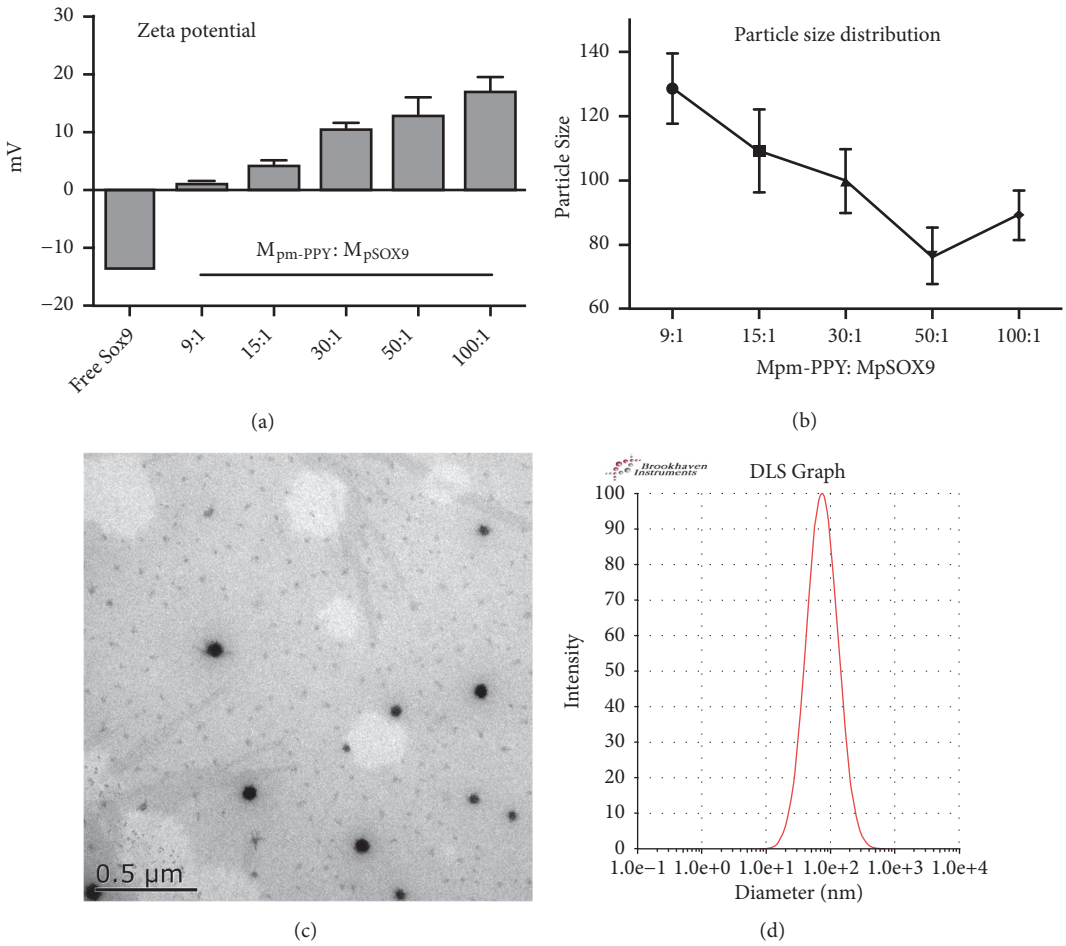

Figure 3: Characterizations of pmPPY/pSox9 nanoparticles. *Notes.* (a) Zeta-potential measurement, Lane1: Lipofectamine 2000-pSox9; Lane (2-6): pSox9/pmPPY nanoparticles in ratios of 9:1, 15:1, 30:1, 50:1, and 100:1; (b) particle size distribution; (c) Transmission Electron Microscope (TEM) image of pmPPY/pSox9 nanoparticles (50:1) (scale length: 500 nm); (d) dynamic light scattering (DLS) analysis of pmPPY/pSox9 nanoparticles (50:1).

3.4. Cytotoxicity Assay. The cytotoxicity of nanoparticles (weight ratios of pmPPY/pSox9: 9:1, 15:1, 30:1, 50:1, 100:1, 150:1, 200:1, and 300:1) was evaluated against Lipofectamine^{TM} 2000 and PEI (25kDa). As shown in Figure 2, the cell viability results showed significant differences between Lipofectamine^{TM} 2000/pSox9 (≈ 60.0 %) and the other pmPPY/pSox9 nanoparticles (> 90.0 %), $p<0.05$. The complex to certain extent displayed some level of toxicity with increasing load of pmPPY. In addition, the PEI (25kDa) /pSox9 group displayed a continuous increase in cell viability with a reduction in the PEI concentration.

3.5. Characterization of pSox9/pmPPY Complex. Based on the results of gel retardation and cytotoxicity assay, pmPPY-pSox9 prepared at 5 different M_{pmPPY}/M_{pSox9} ratios (9:1, 15:1, 30:1, 50:1, and 100:1) were characterized by Zeta potential measurement, transmission electron microscopy (TEM), and dynamic light scanning (DLS).

3.5.1. Zeta Potential Measurement. Zeta potential measurement is a common way to analyze the ability of a gene carrier to combine with negatively charged plasmid. Compared with free plasmid Sox9, ethylenediamine modified PPY (as Figure 3(a) indicates) displayed a positive charge value of 20.52 ± 1.26 mV. Meanwhile, the nanoparticles prepared at five different pmPPY/pSox9 weight ratios (9:1, 15:1, 30:1, 50:1, and 100:1) exhibited an incremental Zeta potential from 0.51 ± 0.12 mV to 14.51 ± 1.28 mV as the weight ratio increased.

3.5.2. Morphology and Particle Size Distribution. The result of DLS analyses was shown in Figure 3(b). The pmPPY-pSox9 prepared at a weight ratio of 50:1 displayed a lower nanoparticle size than other tested groups, which indicates that the pmPPY-pSox9 nanoparticles at this ratio might be potential gene carriers owing to their small particle size. As depicted in Figure 3(c), pmPPY/pSox9 nanoparticles (50:1) were well dispersed and generally uniformed in size less than 100 nm. The result was consistent with the measurements made by DLS, which revealed the particle size of pmPPY/pSox9 complex with an average diameter of 76.64 nm (Figure 3(d)). The pmPPY-pSox9 nanoparticles prepared at a pmPPY/pSox9 weight ratio of 50:1 exhibited a uniform

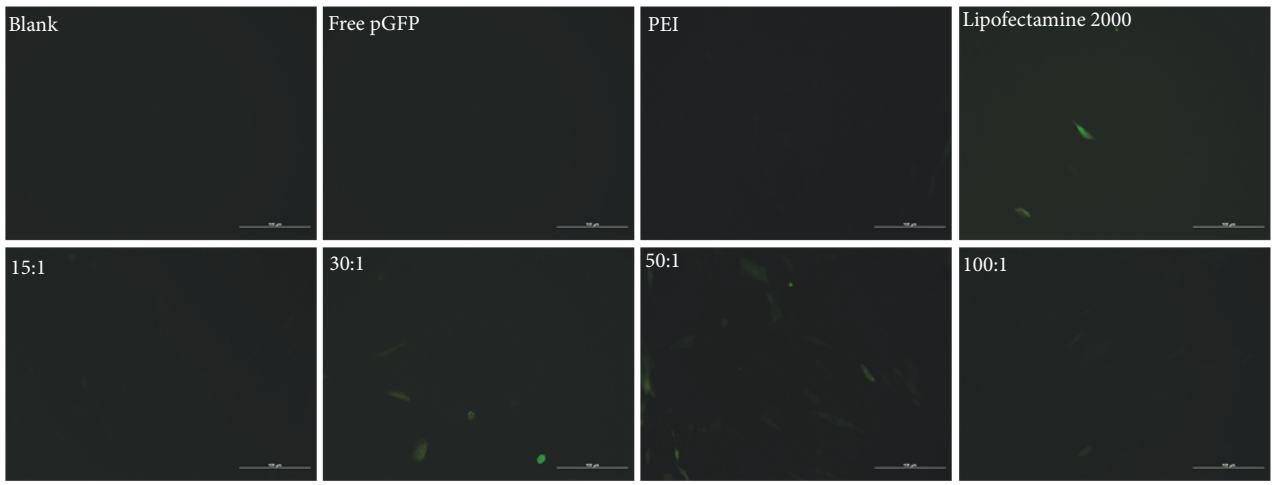

Figure 4: GFP transfection. Notes: Blank: 3T6 cells treated with only pm-PPY; free pGFP: 3T6 cells transfected with only GFP plasmid; Lipofectamine 2000: 3T6 cells transfected with Lipofectamine 2000-pGFP nanoparticles; 15:1: 3T6 cells transfected with pm-PPY-pGFP at a weight ratio of 15:1; 30:1: 3T6 cells transfected with pm-PPY-pGFP at a weight ratio of 30:1; 50:1: 3T6 cells transfected with pm-PPY-pGFP at a weight ratio of 50:1; 100:1: 3T6 cells transfected with pm-PPY-pGFP at a weight ratio of 100:1.

spherical shape, which may be conducive to cell endocytosis during transfection.

3.6. Transfection Efficiency Assay

3.6.1. pGFP Transfection. The result of pGFP transfection was analyzed by fluorescence microscopy (TI-U; Nikon, Tokyo, Japan). From Figure 4, it was clear that the fluorescence intensity reached a maximum when pmPPY/pGFP weight ratio was at 50:1. Meanwhile, other 2 nanoparticles groups (30:1 and 100:1) displayed comparable fluorescence intensity with Lipofectamine 2000 transfected group.

3.6.2. Enzyme-Linked Immunosorbent Assay and RT-PCR Test. As demonstrated in Figure 5(a), the 50:1 group gave the highest transfection effect (535.13pg/ml) among other tested groups, which was 2.7-fold greater than the blank (148.55pg/ml). However, compared to Lipofectamine 2000 group, the 50:1 category showed high significant level of Sox9 expression ($P=0.0346$). The result of RT-PCR (Figure 5(b)) showed the same trend with ELISA assay.

3.6.3. Western Blot Analysis. Ultimately, the intracellular expression of Sox9 was analyzed by Western blotting (Figure 5(c)). Based on a previous study, pmPPY-pSox9 nanoparticles at a weight ratio of 15:1, 30:1, 50:1, and 100:1 were selected for transfection efficiency measurements conducted by western blot. The protein level of Sox9 in Lane 7 (pSox9/pmPPY-1:50) was significantly higher than the other groups ($p<0.05$). Lipofectamine^{TM} 2000 and polyetherimide (PEI) groups expressed greater Sox9 protein levels (Lanes 3 and 4, resp.) than the control groups (pmPPY-treated group, Lane 1; and free plasmid Sox9 treated group Lane 2).

3.7. Identification of Chondroblasts

3.7.1. Staining Analysis of Induced Chondrogenesis. Normal chondrocytes showed higher levels of proteoglycans and peroxidase expressions [32–34]. Therefore, the staining analysis explored these unique features in the induced MEF cells to evaluate the level of chondrogenesis (Figure 6). The toluidine blue staining of both induced MEF cells (Figure 6(d)) and chondrocytes (Figure 6(g)) was partially purple in color (except the nucleus) showing the formation of proteoglycans, which was clearly blue in the normal MEF cells (Figure 6(a)). Similarly, the Safranin O staining of both induced MEF (Figure 6(e)) and chondrocytes (Figure 6(h)) showed deeply colored cells, which were different from the normal MEF (Figure 6(b)). The result of the immunofluorescence staining showed positive expression of collagen type II in both induced MEF cells (Figure 6(f)) and chondrocytes (Figure 6(i)).

3.7.2. Western Blotting Assay. Western Blot analysis was used to determine the level of expression of collage type II protein in MEF cells in this study. In Figure 7, the level of collage type II protein in the pmPPY/pSox9 induced MEF cells were significantly higher than that in untreated MEF cells ($p<0.05$). Meanwhile, the levels of expression of collagen type II showed no significant difference in chondrocytes and induced MEFs groups ($P=0.8079$).

3.7.3. Morphology Observation and GAG Production. As Figure 8(a) showed, the induced MEFs exhibited polygon morphology at 21 days past seeding (14 days after last transfection). Correspondingly, in Figure 8(b), untreated MEFs showed the lowest GAG secretion of all the groups. In induced-MEFs group, GAG secretion is continuously ascending as the extension of time. At 18 days past seeding, the GAG

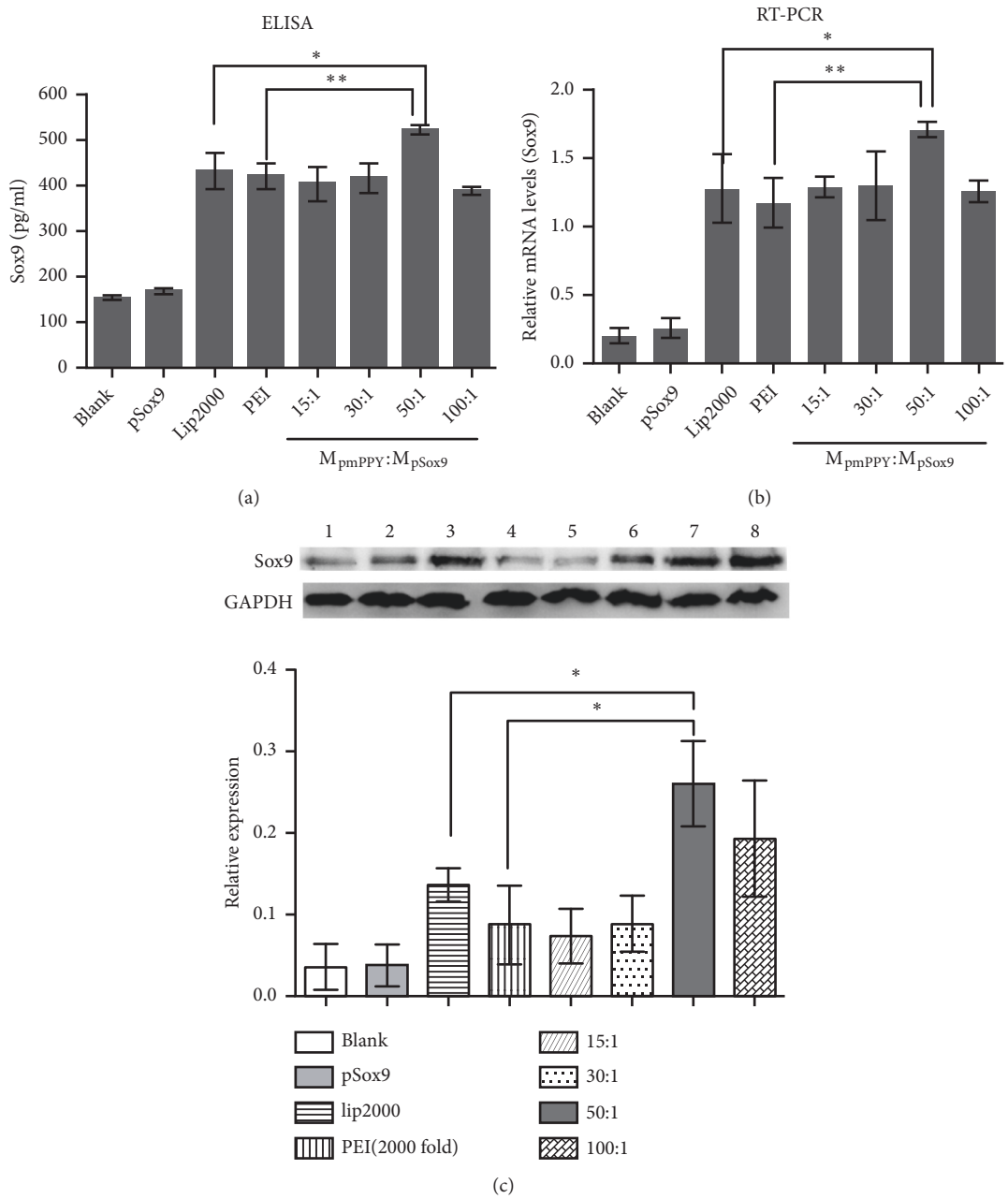

Figure 5: Gene transfection efficiency analyses. *Notes.* (a) Enzyme-linked immunosorbent assay (ELISA): Lane 1: Blank (cells treated with pmPPY only), Lane 2: Free plasmid Sox9, Lane 3: PEI/pSox9 (2000-folds of dilution), Lane 4: Lipofectamine 2000 /pSox9, Lane 5-8: pSox9/pmPPY nanoparticles in ratios of 15:1, 30:1, 50:1, and 100:1;(b) RT-PCR, Lane 1: Blank (cells treated with pmPPY only), Lane 2: Free plasmid Sox9, Lane 3: PEI/pSox9 (2000-folds of dilution), Lane 4: Lipofectamine 2000 /pSox9, Lane 5-8: pSox9/pmPPY nanoparticles in ratios of 15:1, 30:1, 50:1, and 100:1 (c) Western Blot, Lane (1-4): Blank (cells treated with pmPPY only), Free plasmid Sox9, Lipofectamine 2000 /pSox9, PEI (2000-fold dilution)/pSox9, Lane 5-8, pmPPY-pSox9 nanoparticles prepared at different weight ratios 15:1, 30:1, 50:1, and 100:1, from left to right; and a quantitative analysis of the relative expression levels of Sox9 (mean±standard deviation of measurements from three replicates) $*P<0.05$, $**P<0.01$.

secretion showed no statistical significance between induced-MEFs group and primary chondrocytes group (P=0.85).

3.7.4. Reprogramming Efficiency Assay. The reprogramming efficiency was evaluated by FACS analysis, In Figure 9(b), the collagen II+ cells was about 77.4%, which can roughly represent the reprogramming efficiency.

4. Discussions

4.1. Electrophoresis Assay. Generally, negatively charged free plasmids are not taken up to any significant degree by cells due to the nature of cell membranes. Several studies have therefore been directed at finding an excellent vector to carry such plasmids into target cells. In this regard, polysaccharide

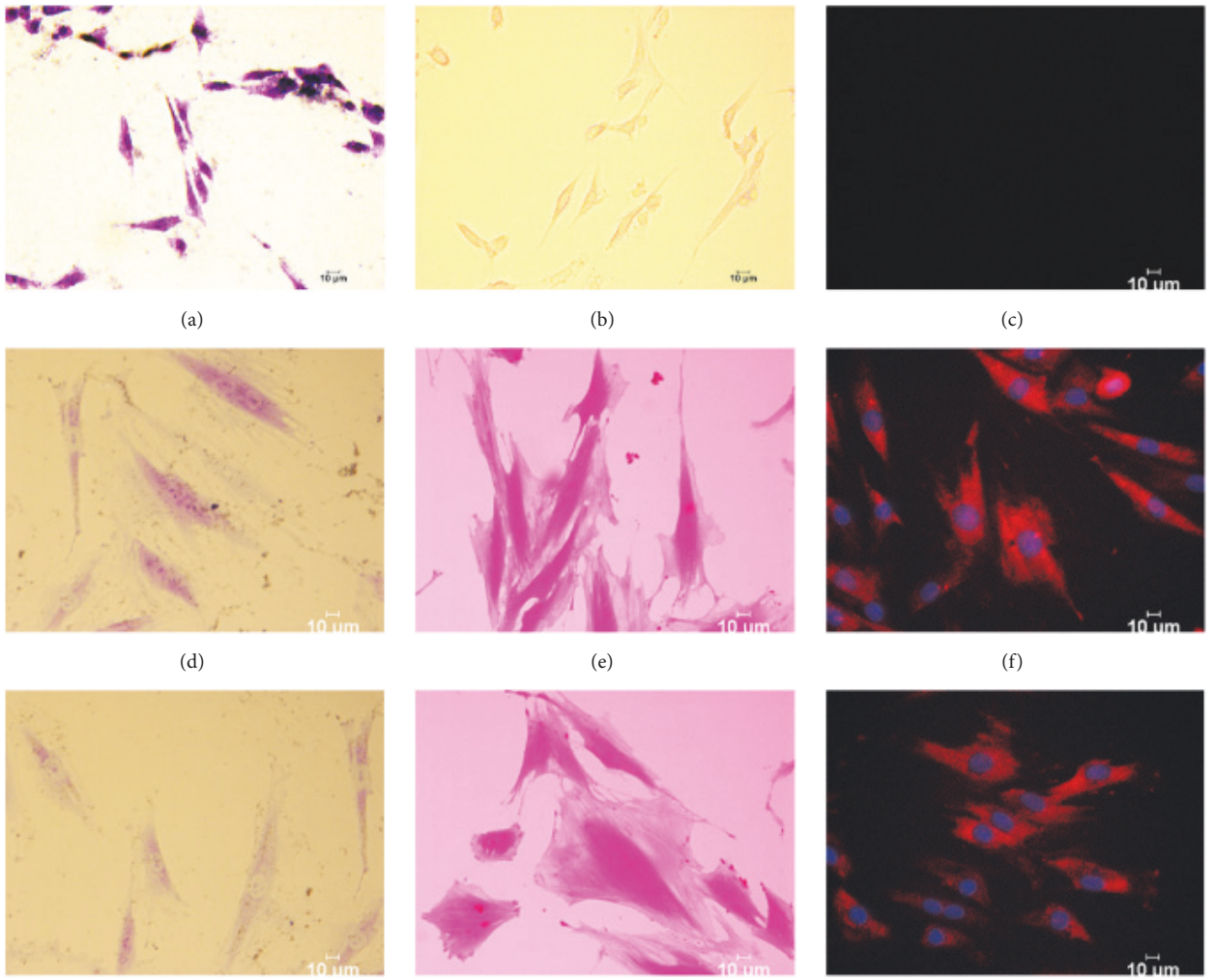

FIGURE 6: Staining of MEF cells: (a-c) MEF cells treated with pm-PPY; (d-f) Induced-MEF cells; (g-i): Chondrocytes. (a), (d), and (g) Toluidine blue staining. (b), (e), and (h) Safranine O staining. (c), (f), and (i) Immunofluorescence staining of collagen type II.

(as a natural product) has drawn worldwide attention due to its unique structural properties of polyhydroxyl groups that make it easy to be modified into the cationic form. The electrophoretic results showed that the increasing cationic nature of the pmPPY/pSox9 nanoparticles succeeded in retarding the migration of the plasmid. This implies that the PEI-modified polysaccharide from *Porphyra yezoensis* was very efficient in coating the plasmid Sox9, which might play a significant role in cellular uptake [24].

4.2. Cytotoxicity of pmPPY-Sox9 Nanoparticles. The cytotoxicity of cationic polymers is known to depend on their surface charge: excess positive charges on the nanoparticles surface can interact with and functionally impaired certain cellular components [35]. In this study, all the tested groups depicted lower cytotoxicity than the Lipofectamine 2000, which illustrate that those pmPPY-Sox9 nanoparticles could be developed into safe nonviral gene carriers. However, 2 groups of pm-PPY-Sox9 nanoparticles (9:1 and 50:1) showed slightly higher cell viability than 100%, which could be due to experimental errors. In addition, the plasmid DNA cannot be retarded when the fold of dilution of PEI exceeded 2000 (data not shown). Therefore, the folds of dilution of PEI were selected below 2000-fold in cytotoxicity assay. All the PEI-Sox9 groups showed remarkable cytotoxicity (cell viability < 70%), indicating that PEI might not be an ideal gene carrier for 3T6 cells transfection.

4.3. Instrumental Assay. The characterization of gene carriers was always considered as a tentative study of cellular uptake capacity. The Zeta potentials of nanoparticles (NPs) determine their colloidal stability and influence the effectiveness of their interactions with negatively charged cell membranes. Therefore, the Zeta potentials of NPs can strongly affect their transfection efficiencies [36]. The Zeta potential measurement revealed that the amount of pmPPY is directly

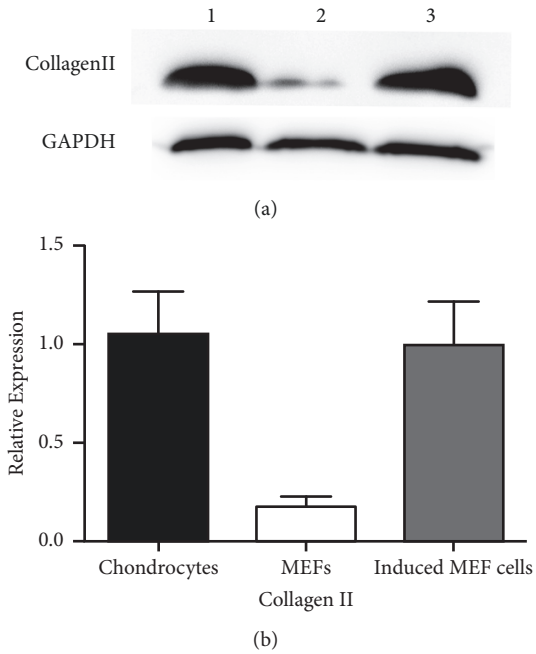

Figure 7: Col2α1 expression measurement: (a) Western blot, Lane 1: induced MEF cells, Lane 2: MEF cells treated with pmPPY only. (b) A quantitative analysis of the relative expression levels of Col2α1 (mean±standard deviation of measurements from three replicates) $**P<0.01$.

related to surface charge of pmPPY/pSox9 nanoparticles. Particle size plays a key role in the cellular uptake of NPs and is thus one of the most important parameters for cationic polymers intended for application as gene vectors. Several previous studies reported that cells typically take up NPs ranging from about 50 to several hundred nanometers [37, 38]. In accordance with our progress on polysaccharide nonviral gene delivery system, different weight ratios of polysaccharide and plasmid DNA result in different particle size. In general, increased weight ratios of cationic polymer and plasmid DNA possess higher Zeta potentials owing to accumulation of positive charge. Brain A. Sanderson et al. [39] proved that higher charge density and particle size could result in a promising percentage of DNA binding. However, when it comes to nonviral gene delivery system, the cytotoxicity is another nonnegligible factor. Based on our research works [15, 40–42], there is always a weight ratio of cationic polymer and plasmid DNA among others to form smallest particle size of nanoparticles. The gene-loaded nanoparticles that display best gene transfer efficiency distribute in or around this ratio. In this study, the particle size of pmPPY-pSox9 nanoparticles at a weight ratio of 50:1 was lower than other tested groups. Taking Zeta potential measurement into consideration, the reason for the particle size increase is that low surface charge might result in a loose connection between pmPPY and pSox9; meanwhile, when surface charge increased, their mutual repulsion and the permeation of water and hydrated counter-ions needed to neutralize these charges would then cause swelling, thereby increasing the NP diameters [43].

4.4. Gene Transfection Efficiency. Green fluorescence protein (GFP) is a common reporter gene for visually investigating gene transfection efficiency. Obviously, the result of GFP transfection was consistent with ELISA and RT-PCR test. However, the difference between Lip2000 group and 50:1 group in WB test is more significant than that in ELISA. This is probably because of the detachment of MEFs caused by Lipofectamine 2000 with its higher toxicity. Although the supernatant was centrifuged before applying to ELISA test, some intracellular Sox9 protein might inevitably be released into the supernatant. In accordance with our previous analysis, we can draw the conclusion that a nanoparticle that possessed a proper size and uniform spherical shape might give rise to high gene transfection efficiency through cell endocytosis during transfer [44, 45].

4.5. Direct Reprogramming of MEFs into Chondrocytes. MEFs are one of the best available cell populations for tissue engineering since the iPSCs introduction. Compared to MEFs with spindle shape in morphology, chondrocytes are polygonal and express collagen proteins. Thus, collagen II is always considered as a biomarker for cell line identification. In this study, the results of the staining analysis and immunofluorescence revealed that the induced MEFs express high levels of proteoglycans and collagen II. Additionally, morphology observation showed that, at 21 days after seeding (about 14 days after the last transfection, Figure 8(a)), the induced MEFs tended to polygonal shape from spindle shape. All these results indicated that the induced MEFs were similar to chondrocytes from both morphology and biological property. Thus, we selected the induced MEFs at 14th day after last transfection for chondrocyte identification when the induced MEFs showed chondrocytes-like morphology. During the reprogramming process, the chondrocytes differentiation medium was changed every 48h to prevent induced MEFs from converting to other cell lines except chondrocytes. In addition, both of the induced MEFs and primary chondrocytes showed limited proliferative capacity (2 passages before senescence versus 3 passages of that in primary chondrocytes). This result might illustrate that the induced MEFs are terminally differentiated cells. These findings indicate that pmPPY-pSox9 nanoparticles could be a promising gene carrier for the direct reprogramming of MEFs to chondrocytes.

5. Conclusion

For the first time in this study, we have established a single-gene strategy for the generation of chondrocytes through polysaccharide-based nonviral gene delivery system. The prepared pmPPY exhibited low cytotoxicity and high transfection efficiency in mouse embryo fibroblasts (MEFs), which finally drove the successful reprogramming of MEFs into chondrocytes. This research enriched cell lineage for the repair of articular cartilage. Additionally, it offered some academic bases and references for the applications of marine polysaccharide in gene delivery system and tissue engineering. More comprehensive mechanisms of chondrocyte reprogramming as well as in vivo transplantation experiments to

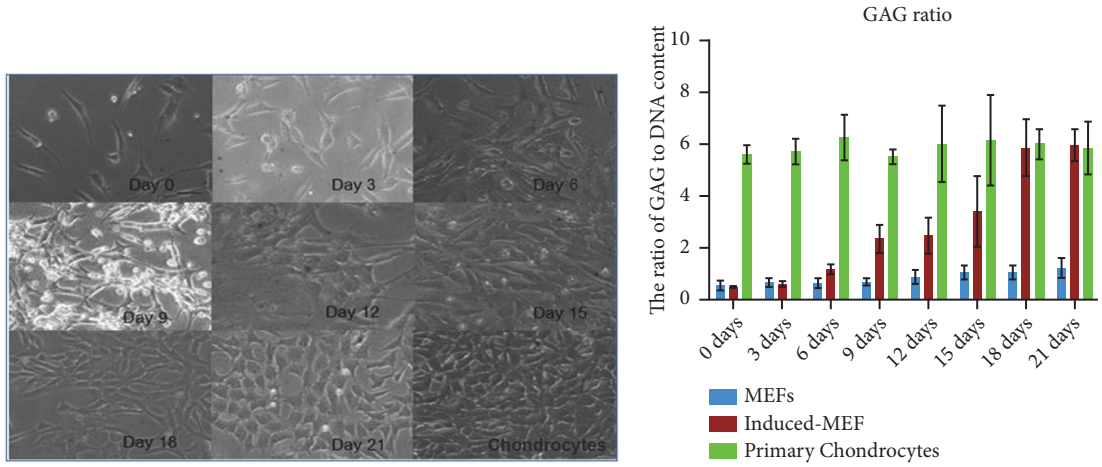

(a) (b)

Figure 8: Morphology observation and GAG production: (a) Morphology of induced MEFs from day 0 to day 21 and primary chondrocytes; (b) GAG production of untreated MEFs (blue bar), induced MEFs (red bar), and primary chondrocytes (green bar) from day 0 to day 21.

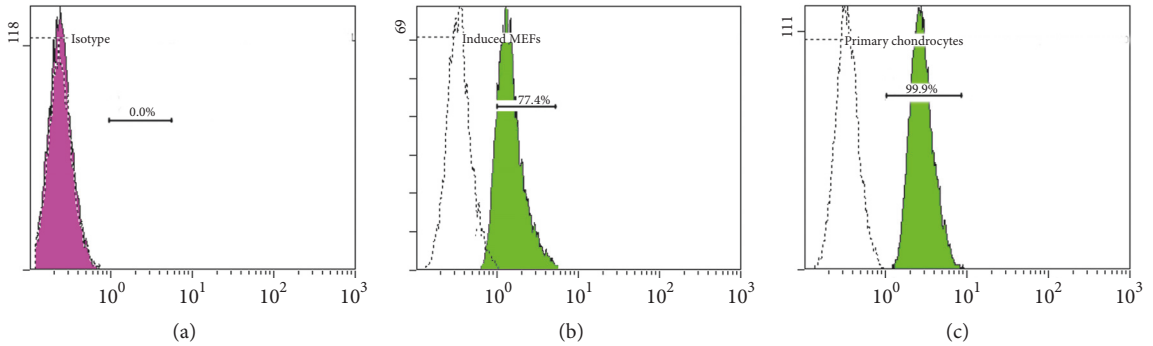

(a) (b) (c)

Figure 9: Reprogramming efficiency: (a) Isotype group; (b) induced MEFs group; (c) primary chondrocytes group.

confirm the function of induced MEFs shall be the topic of future investigation.

Data Availability

The preparation procedure of pmPPY is included within the supplementary information. The AFM (Atomic Force Microscope) data used to characterize the advanced structure of pmPPY is included within the supplementary information. The 1H-HMR data were used to illustrate modification pmPPY. The data result from western blot, Elisa, immunofluorescences, and chemical staining used to support the findings of this study are included within the article.

Disclosure

Dr. Qingtong Yu is the first author. Yan Wang is the co-first author. Xia Cao, Wenwen Deng, and Michael Adu Frimpong are coauthors.

Conflicts of Interest

The authors declare no conflicts of interest in this work.

Authors' Contributions

Qingtong Yu and Yan Wang contributed equally to this work.

Acknowledgments

This work was supported by National Natural Science Foundation, China (81473172, 81503025, 81773695, 81720108030, and 81273470), Doctoral Fund of Ministry of Education of China (20123227110009), Special Funds for 333 projects (BRA2013198), and Industry-University-Research Institution Cooperation (JHB2012-37, GY2012049, GY2013055) in Jiangsu Province and Zhenjiang City. This work was also supported by senior professionals' foundation of Jiangsu University projects (13JDG007) and A Project Funded by the Priority Academic Program Development of Jiangsu Higher Education Institutions. Meanwhile, Jiangsu Province

Postdoctoral Foundation (1701068C) and China Postdoctoral Foundation (2017M621659) were also involved in this research work.

Supplementary Materials

Supplementary Figure 1 illustrated the structure of Sox 9 plasmid used in this study. Supplementary Figure 2 is the 1H-NMR analysis of PPY before and after cationization. Supplementary Figure 3 is the atonic force microscopy result of pmPPY. In addition, the preparation of pmPPY was also listed in supplementary information. *(Supplementary Materials)*

References

[1] K. Takahashi and S. Yamanaka, "Induction of pluripotent stem cells from mouse embryonic and adult fibroblast cultures by defined factors," *Cell*, vol. 126, no. 4, pp. 663–676, 2006.

[2] N. Tsumaki, M. Okada, and A. Yamashita, "iPS cell technologies and cartilage regeneration," *Bone*, vol. 70, pp. 48–54, 2015.

[3] K. Si-Tayeb, F. K. Noto, M. Nagaoka et al., "Highly efficient generation of human hepatocyte–like cells from induced pluripotent stem cells," *Hepatology*, vol. 51, pp. 297–305, 2010.

[4] S. Mae and K. Osafune, "Kidney regeneration from human induced pluripotent stem cells," *Current Opinion in Organ Transplantation*, vol. 20, no. 2, pp. 171–177, 2015.

[5] S. Pellegrini, F. Ungaro, A. Mercalli et al., "Human induced pluripotent stem cells differentiate into insulin-producing cells able to engraft in vivo," *Acta Diabetologica*, vol. 52, no. 6, pp. 1025–1035, 2015.

[6] S. Karumbayaram, B. G. Novitch, M. Patterson et al., "Directed differentiation of human-induced pluripotent stem cells generates active motor neurons," *Stem Cells*, vol. 27, no. 4, pp. 806–811, 2009.

[7] J. S. Wendel, L. Ye, R. Tao et al., "Functional effects of a tissue-engineered cardiac patch from human induced pluripotent stem cell-derived cardiomyocytes in a rat infarct model," *Stem Cells Translational Medicine*, vol. 4, no. 11, pp. 1324–1332, 2015.

[8] M. Ieda, J. D. Fu, P. Delgado-Olguin et al., "Direct reprogramming of fibroblasts into functional cardiomyocytes by defined factors," *Nihon Rinsho Japanese Journal of Clinical Medicine*, vol. 69, supplement 7, pp. 524–527, 2011.

[9] J. A. Efe, S. Hilcove, J. Kim et al., "Conversion of mouse fibroblasts into cardiomyocytes using a direct reprogramming strategy," *Nature Cell Biology*, vol. 13, no. 3, pp. 215–222, 2011.

[10] J. Kim, J. A. Efe, S. Zhu et al., "Direct reprogramming of mouse fibroblasts to neural progenitors," *Proceedings of the National Acadamy of Sciences of the United States of America*, vol. 108, no. 19, pp. 7838–7843, 2011.

[11] P. G. Coune, B. L. Schneider, and P. Aebischer, "Parkinson's disease: gene therapies," *Cold Spring Harbor Perspectives in Medicine*, vol. 2, no. 4, Article ID a009431, 2012.

[12] M. A. Dergunova, T. V. Alexeenko, S. Y. Zhanaeva et al., "Characterization of the novel chemically modified fungal polysaccharides as the macrophage stimulators," *International Immunopharmacology*, vol. 9, no. 6, pp. 729–733, 2009.

[13] W. W. Deng, X. Cao, M. Wang et al., "Delivery of a transforming growth factor β-1 plasmid to mesenchymal stem cells via cationized Pleurotus eryngii polysaccharide nanoparticles," *International Journal of Nanomedicine*, vol. 7, pp. 1297–1311, 2012.

[14] M. Wang, W. Deng, M. Fu et al., "Efficient gene transfer into rat mesenchymal stem cells with cationized Lycium barbarum polysaccharides nanoparticles," *Carbohydrate Polymers*, vol. 86, no. 4, pp. 1509–1518, 2011.

[15] W. Deng, M. Fu, Y. Cao et al., "Angelica sinensis polysaccharide nanoparticles as novel non-viral carriers for gene delivery to mesenchymal stem cells," *Nanomedicine: Nanotechnology Biology & Medicine*, vol. 9, no. 8, pp. 1181–1191, 2013.

[16] S. Cao, S. Yu, Y. Chen et al., "Chemical reprogramming of mouse embryonic and adult fibroblast into endoderm lineage," *The Journal of Biological Chemistry*, vol. 292, no. 46, pp. 19122–19132, 2017.

[17] T. Ikeda, S. Kamekura, A. Mabuchi et al., "The combination of SOX5, SOX6, and SOX9 (the SOX trio) provides signals sufficient for induction of permanent cartilage," *Arthritis & Rheumatology*, vol. 50, no. 11, pp. 3561–3573, 2004.

[18] H. Akiyama, M. C. Chaboissier, J. F. Martin, A. Schedl, and B. de Crombrugghe, "The transcription factor Sox9 has essential roles in successive steps of the chondrocyte differentiation pathway and is required for expression of Sox5 and Sox6," *Genes & Development*, vol. 16, no. 21, pp. 2813–2828, 2002.

[19] M. Kadaja, B. E. Keyes, M. Lin et al., "SOX9: a stem cell transcriptional regulator of secreted niche signaling factors," *Genes & Development*, vol. 28, no. 4, pp. 328–341, 2014.

[20] Y. Yi, H. Yu, G. Qian, and W. Qiong, "A tetracycline expression system in combination with Sox9 for cartilage tissue engineering," *Biomaterials*, vol. 35, no. 6, pp. 1898–1906, 2014.

[21] C. Cournil-Henrionnet, C. Huselstein, Y. Wang et al., "Phenotypic analysis of cell surface markers and gene expression of human mesenchymal stem cells and chondrocytes during monolayer expansion," *Biorheology*, vol. 45, no. 3-4, pp. 513–526, 2008.

[22] J. S. Park, H. N. Yang, D. G. Woo et al., "Chondrogenesis of human mesenchymal stem cells mediated by the combination of SOX trio SOX5, 6, and 9 genes complexed with PEI-modified PLGA nanoparticles," *Biomaterials*, vol. 32, no. 14, pp. 3679–3688, 2011.

[23] J. Cao, S. Wang, C. Yao, Z. Xu, and X. Xu, "Hypolipidemic effect of porphyran extracted from Pyropia yezoensis in ICR mice with high fatty diet," *Journal of Applied Phycology*, vol. 28, no. 2, pp. 1315–1322, 2015.

[24] Q. Yu, J. Cao, B. Chen et al., "Efficient gene delivery to human umbilical cord mesenchymal stem cells by cationized Porphyra yezoensis polysaccharide nanoparticles," *International Journal of Nanomedicine*, vol. 10, pp. 7097–7107, 2015.

[25] E. J. Wallenstein, J. Barminko, R. S. Schloss, and M. L. Yarmush, "Serum starvation improves transient transfection efficiency in differentiating embryonic stem cells," *Biotechnology Progress*, vol. 26, no. 6, pp. 1714–1723, 2010.

[26] B. Johnstone, T. M. Hering, A. I. Caplan et al., "In vitro chondrogenesis of bone marrow-derived mesenchymal progenitor cells," *Experimental Cell Research*, vol. 238, no. 1, pp. 265–272, 1998.

[27] M. B. Mueller, T. Blunk, B. Appel et al., "Insulin is essential for in vitro chondrogenesis of mesenchymal progenitor cells and influences chondrogenesis in a dose-dependent manner," *International Orthopaedics*, vol. 37, no. 1, pp. 153–158, 2013.

[28] D. A. Grande, J. Mason, E. Light, and D. Dines, "Stem cells as platforms for delivery of genes to enhance cartilage repair," *Journal of Bone and Joint Surgery*, vol. 85-A, supplement 2, pp. 111–116, 2003.

[29] L. Kupcsik, M. J. Stoddart, Z. Li, L. M. Benneker, and M. Alini, "Improving chondrogenesis: potential and limitations of sox9

gene transfer and mechanical stimulation for cartilage tissue engineering," *Tissue Engineering Part: A*, vol. 16, no. 6, pp. 1845–1855, 2010.

[30] M. S. Huh, E. J. Lee, H. Koo et al., "Polysaccharide-based nanoparticles for gene delivery," *Topics in Current Chemistry*, vol. 375, article 31, 2017.

[31] F. M. Kievit, O. Veiseh, N. Bhattarai et al., "PEI-PEG-chitosan-copolymer-coated iron oxide nanoparticles for safe gene delivery: synthesis, complexation, and transfection," *Advanced Functional Materials*, vol. 19, no. 14, pp. 2244–2251, 2009.

[32] R. Jin, L. S. Moreira Teixeira, P. J. Dijkstra et al., "Enzymatically-crosslinked injectable hydrogels based on biomimetic dextran-hyaluronic acid conjugates for cartilage tissue engineering," *Biomaterials*, vol. 31, no. 11, pp. 3103–3113, 2010.

[33] J. B. Catterall, A. D. Rowan, S. Sarsfield, J. Saklatvala, R. Wait, and T. E. Cawston, "Development of a novel 2D proteomics approach for the identification of proteins secreted by primary chondrocytes after stimulation by IL-1 and oncostatin M," *Rheumatology*, vol. 45, no. 9, pp. 1101–1109, 2006.

[34] B. H. Min, H. J. Kim, H. Lim, and S. R. Park, "Characterization of subpopulated articular chondrocytes separated by Percoll density gradient," in *In Vitro Cellular & Developmental Biology - Animal*, vol. 38, pp. 35–40, 2002.

[35] H. J.-P. Ryser, "A membrane effect of basic polymers dependent on molecular size," *Nature*, vol. 215, no. 5104, pp. 934–936, 1967.

[36] B. Xiao, Y. Wan, X. Wang et al., "Synthesis and characterization of N-(2-hydroxy)propyl-3-trimethyl ammonium chitosan chloride for potential application in gene delivery," *Colloids and Surfaces B: Biointerfaces*, vol. 91, pp. 168–174, 2012.

[37] Y. Song, Y. Sun, X. Zhang, J. Zhou, and L. Zhang, "Homogeneous quaternization of cellulose in NaOH/Urea aqueous solutions as gene carriers," *Biomacromolecules*, vol. 9, no. 8, pp. 2259–2264, 2008.

[38] Y. Liu and T. M. Reineke, "Hydroxyl stereochemistry and amine number within poly(glycoamidoamine)s affect intracellular DNA delivery," *Journal of the American Chemical Society*, vol. 127, no. 9, pp. 3004–3015, 2005.

[39] B. A. Sanderson, D. S. Sowersby, S. Crosby, M. Goss, L. K. Lewis, and G. W. Beall, "Charge density and particle size effects on oligonucleotide and plasmid DNA binding to nanosized hydrotalcite," *Biointerphases*, vol. 8, no. 8, pp. 1–11, 2013.

[40] W. W. Deng, X. Cao, M. Wang et al., "Efficient gene delivery to mesenchymal stem cells by an ethylenediamine-modified polysaccharide from mulberry leaves," *Small*, vol. 8, no. 3, pp. 441–445, 2012.

[41] X. Cao, W. Deng, R. Qu et al., "Non-viral co-delivery of the four yamanaka factors for generation of human induced pluripotent stem cells via calcium phosphate nanocomposite particles," *Advanced Functional Materials*, vol. 23, no. 43, pp. 5403–5411, 2013.

[42] C. Xia, W. Deng, W. Yuan et al., "Encapsulation of plasmid DNA in calcium phosphate nanoparticles: stem cell uptake and gene transfer efficiency," *International Journal of Nanomedicine*, vol. 6, pp. 3335–3349, 2011.

[43] B. Xiao, P. Ma, L. Ma et al., "Effects of tripolyphosphate on cellular uptake and RNA interference efficiency of chitosan-based nanoparticles in Raw 264.7 macrophages," *Journal of Colloid and Interface Science*, vol. 490, pp. 520–528, 2017.

[44] X. Xu, R. M. Capito, and M. Spector, "Plasmid size influences chitosan nanoparticle mediated gene transfer to chondrocytes," *Journal of Biomedical Materials Research Part A*, vol. 84A, no. 4, pp. 1038–1048, 2010.

[45] F. C. MacLaughlin, R. J. Mumper, J. Wang et al., "Chitosan and depolymerized chitosan oligomers as condensing carriers for in vivo plasmid delivery," *Journal of Controlled Release*, vol. 56, no. 1–3, pp. 259–272, 1998.